



This is a repository copy of *Post-fire residual mechanical properties of Q460GJ steel under different pre-tensile stresses*.

White Rose Research Online URL for this paper:

<https://eprints.whiterose.ac.uk/219317/>

Version: Accepted Version

Article:

Li, S., Li, A., Wang, W. et al. (1 more author) (2024) Post-fire residual mechanical properties of Q460GJ steel under different pre-tensile stresses. *Fire Safety Journal*, 150 (Part B). 104280. ISSN 0379-7112

<https://doi.org/10.1016/j.firesaf.2024.104280>

© 2024 The Authors. Except as otherwise noted, this author-accepted version of a journal article published in *Fire Safety Journal* is made available via the University of Sheffield Research Publications and Copyright Policy under the terms of the Creative Commons Attribution 4.0 International License (CC-BY 4.0), which permits unrestricted use, distribution and reproduction in any medium, provided the original work is properly cited. To view a copy of this licence, visit <http://creativecommons.org/licenses/by/4.0/>

Reuse

This article is distributed under the terms of the Creative Commons Attribution (CC BY) licence. This licence allows you to distribute, remix, tweak, and build upon the work, even commercially, as long as you credit the authors for the original work. More information and the full terms of the licence here:

<https://creativecommons.org/licenses/>

Takedown

If you consider content in White Rose Research Online to be in breach of UK law, please notify us by emailing eprints@whiterose.ac.uk including the URL of the record and the reason for the withdrawal request.



eprints@whiterose.ac.uk
<https://eprints.whiterose.ac.uk/>

1 **Post-fire residual mechanical properties of Q460GJ steel** 2 **under different pre-tensile stresses**

3 *Siqi Li^a, Aibing Li^a, Weiyong Wang^{a, b*}, Shan-Shan Huang^c*

4 *a School of Civil Engineering, Chongqing University, Chongqing 400045, P. R. China*

5 *b Key Laboratory of New Technology for Construction of Cities in Mountain Area (Ministry of Education),*

6 *Chongqing University, Chongqing 400045, P. R. China*

7 *c Department of Civil and Structural Engineering, The University of Sheffield, Sir Frederick Mappin Building,*

8 *Mappin Street, Sheffield S1 3JD, UK*

9 **Abstract:** Previous studies on the post-fire mechanical properties of steel were
10 conducted with unstressed state, without considering the influence of pre-stress which
11 subjected to structures in reality. In this article, the post-fire residual mechanical
12 properties of Q460GJ steel under different pre-tensile stresses were studied. The stress-
13 strain curve, elastic modulus, yield strength, ultimate strength and fracture elongation
14 of Q460GJ steel after different elevated temperatures heating are analyzed in detail.
15 The experimental results are compared with that of Q460 steel and S460 steel in the
16 existing literatures. At last, the predictive equations of post-fire mechanical properties
17 of Q460GJ steel under different pre-tensile stresses are established. Q460GJ steel still
18 maintains good ductility after elevated temperature heating, which increases the
19 possibility of reuse of Q460GJ steel element after fire. The Q460GJ steel has better
20 post-fire ductility than that of Q460 and S460 steels. The predictive equations for the
21 post-fire residual mechanical properties for Q460GJ steel under different pre-tensile

* Corresponding Author: W. Wang, Ph.D. & Professor, E-mail: wywang@cqu.edu.cn

22 stresses were proposed. The variation coefficients of yield strength for Q460GJ steel
23 under different pre-tensile stresses after 20 min different elevated temperatures heating
24 were within 0.065. The findings should have a great significance to providing
25 theoretical support for design of reusing or restoring steel building after fire.

26 **Keywords:** Q460GJ steel; Post-fire; Mechanical properties; Stress–strain curve; Reduction factor

27 **1. Introduction**

28 Comparing with traditional concrete building, steel building with applying steel
29 plates or steel sections has the following advanced properties such as light weight, good
30 ductility and better seismic resistance [1-4]. And because the steel components can be
31 manufactured in factory and installed on site while building steel structure, the steel
32 building construction period can be greatly reduced. With long-term consideration, the
33 reusability of steel material can greatly reduce construction waste and make steel
34 building more environmentally friendly [5-8]. Therefore, it is widely adopted by
35 countries around the world and applied in industrial and civil constructions [9-11]. With
36 the continuous improvement of steel manufacture technologies, the control of trace
37 elements in steel production is becoming more and more accurate. Therefore, the
38 mechanical properties of constructional steel, such as yield to strength ratio and
39 ductility could be becoming more and more excellent. The emergence of high-
40 performance structural steel is the inevitable trend of the modern construction industry
41 development [12-14]. High-performance steel has the advantages of high strength and
42 good ductility, which has a good engineering application prospect. Although steel
43 structures have widely recognized advantages such as light weight, good seismic

44 performance and convenient construction, the relatively weak fire resistance of steel
45 structures has still been considered as a major safety hazard [15-18].

46 The elevated temperature caused by fire changes the microstructure of steel, thus
47 changing its mechanical properties. Structural fire safety is one of the key factors in the
48 design of high-rise buildings. Through reasonable fire protection design, the steel
49 structure can withstand fire or elevated temperature for more than 90 minutes without
50 obvious fire resistance loss, so fire or elevated temperature does not always lead to the
51 collapse of the steel structure [19-21]. However, the steel structure after fire will
52 generate residual force and deformation again in the cooling stage and after cooling,
53 which may lead to the insecurity of the structure. In order to reuse or restore the steel
54 building after fire, it is necessary to further evaluate the reliability of steel structures
55 after fire based on the post-fire residual mechanical properties of steel [22-24].
56 Therefore, the study of post-fire residual mechanical properties of steel has become one
57 of the research hotspots in the field of civil engineering, especially the study of post-
58 fire residual mechanical properties of high-performance steel.

59 In order to accurately evaluate the residual performance of steel structure after fire,
60 it is necessary to accurately understand the influence of elevated temperature and
61 cooling process on the mechanical properties of steel after fire [25-27]. In recent years,
62 the researches on mechanical properties of structural steel after fire have been
63 increasing continuously. Qiang et al. [28, 29] conducted tensile tests on high-strength
64 S460, S690 and S960 steels after fire exposure. The test results showed that when the
65 temperature was lower than 600 °C, the mechanical properties of the steels after fire

66 were less affected, while the properties of different grade steels after fire were greatly
67 different. Lee et al. [30] conducted post-fire tensile tests of A992 steel with the elevated
68 temperature range of 200 °C ~1000 °C with water cooling and air cooling modes, and
69 found that, with air cooling mode, the yield strength did not significantly reduce until
70 the elevated temperature exceeded 700 °C. However, with water cooling mode, the
71 yield strength increased and the fracture toughness decreased. Wang et al. [31] studied
72 the mechanical properties of Q460 after fire, and proved that different elevated
73 temperatures and cooling modes have effects on the stress-strain curve, yield strength,
74 tensile strength and fracture elongation of Q460 steel. Zhou et al. [32] compared the
75 mechanical properties of Q690 high-strength steel plates with different thicknesses (10
76 mm and 20 mm) after fire exposure, and found that the mechanical properties
77 deteriorated seriously when the elevated temperatures were higher than 700 °C. Huang
78 et al. [33] conducted post-fire tensile tests for Q690 high-strength steel specimens at
79 three pre-tensile stress ratios of 0.30, 0.55 and 0.80. The experimental results showed
80 that the pre-tensile stress during heating and cooling improved the yield strength and
81 ultimate strength of Q690 steel after fire. However, when the exposure temperature
82 reached 800 °C, the pre-tensile stress has a decreasing effect on the residual strength of
83 Q690 steel after fire. In general, the current research objects were mainly focused on
84 high-strength steel. At the same time, the effect of pre-tensile stress on post-fire residual
85 mechanical properties is the main research direction.

86 **2. Research significance**

87 Without reliable mechanical properties of high-performance steel after fire, the

88 performance evaluation of high-performance steel structure after fire is unreliable [34-
89 36]. As an important basis for evaluating the performance of steel structures after fire,
90 it is of great significance to study the material performance of steel after fire [37-39].
91 At present, there is a lack of evaluation on the mechanical properties of high-
92 performance steel after fire, especially with pre-tensile stress. For example, in 2023,
93 Chinese standard "Steel Plates for Building Structures" (GB/T 19879) [40] was updated
94 to standardize the production and application of high-performance steel, with adding
95 GJ after the original steel grade, such as Q345GJ, commonly known as "GJ steel". GJ
96 steel plate is defined as a high-performance steel plate specially produced for high-rise
97 civil building steel structures. In this article, the post-fire residual mechanical properties
98 of Q460GJ steel with two kinds of plate thickness (8 mm and 12 mm) under different
99 pre-tensile stresses are studied. The stress-strain curve, elastic modulus, yield strength,
100 ultimate strength and fracture elongation of Q460GJ steel after different elevated
101 temperatures heating are analyzed in detail. The experimental results are compared with
102 that of Q460 steel and S460 steel in the existing literatures. At last, the predictive
103 equations of post-fire mechanical properties of Q460GJ steel under different pre-tensile
104 stresses are established. At the same time, the variation coefficient of yield strength of
105 Q460GJ steel under different pre-tensile stresses after different elevated temperatures
106 heating is analyzed based on the Weibull's probability distribution theory. These
107 analyses are used to clarify the uniformity change of Q460GJ steel under different pre-
108 tensile stresses after different elevated temperatures heating. The findings should have
109 a great significance to providing theoretical support for design of reusing or restoring

110 the steel building after fire, and have guiding significance for design, manufacturing,
111 and application of high-performance steel.

112 **3. Post-fire residual mechanical properties test**

113 **3.1 Materials and specimen**

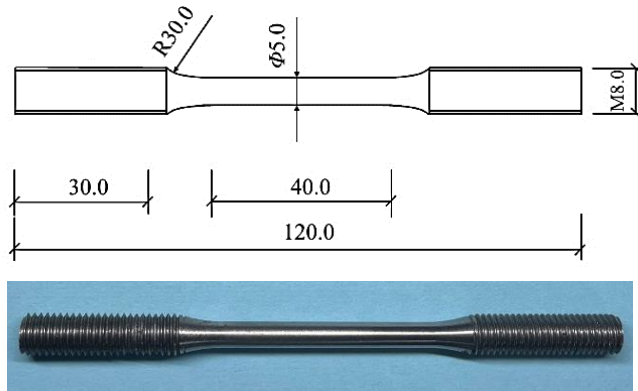
114 The commercial normalized Q460GJ steel plates manufactured according to the
115 Chinese standard GB/T 19879-2023 (Steel plate for building structure) [40] were
116 chosen. Table 1 shows the chemical compositions of the tested Q460GJ steel and the
117 cited Q460 and S460 steels. The 8 mm thickness and 12 mm thickness Q460GJ steel
118 plates were used. The tested specimen was made from the Q460GJ steel plate by wire-
119 electrode cutting with the preparation process meets the requirements of the standards
120 GB/T 228.1-2010(ISO 6892-1:2011) [41] and GB/T228.2-2015(ISO 6892-2:2011)[42].
121 The use of round bar specimens was to maintain the uniformity of specimen dimensions.
122 Figure 1 shows the dimensions and photo image of tested specimen.

123

Table 1 Chemical compositions of Q460GJ steel, Q460 steel and S460 steel.

Steel	Element (wt%)													
	C	Si	Mn	P	S	Al	Cr	Ni	Cu	Mo	Nb	V	Ti	CEV
Q460GJ	0.150	0.320	1.540	0.010	0.0008	0.039	0.050	0.020	0.030	0.004	0.034	0.037	0.003	0.420
Q460[31]	0.070	0.130	0.920	0.012	0.0030	-	-	0.020	-	-	-	-	0.064	0.246
S460[28]	0.172	0.483	1.500	0.012	0.005	0.037	0.020	0.018	-	-	0.046	0.087	0.002	0.447

124



125

126

Fig. 1. Dimensions and photo image of tested specimen (mm).

127

3.2 Heating at elevated temperature with pre-tensile

128

129

130

131

132

133

134

135

136

137

Figure 2 shows the post-fire residual mechanical properties test procedure. The tested specimen was first processed on the electronic high temperature tension measurement, preloaded with a certain tensile stress, then heated to the target temperature, maintained for a period of time, and then naturally cooled to room temperature. The numbers of test specimens and corresponding test conditions are shown in Table 2. The pre-tensile stress was kept through the heating stage and the cooling stage. The pre-tensile stress ratio (γ) was defined as the ratio of the pre-tensile stress (σ) to the yield stress at elevated temperature ($f_{y,T}$). Four stress ratios were designed (0, 0.3, 0.55, 0.8). The yield stresses at elevated temperature of Q460GJ steel plates were tested according to the standards GB/T 228.1-2010 (ISO 6892-1:2011) and

138 GB/T228.2-2015 (ISO 6892-2:2011) and supplied by the Q460GJ steel manufacture.
139 The elevated temperatures chosen were 300 °C, 400 °C, 500 °C, 600 °C, 700 °C, 800 °C
140 and 900 °C, respectively. For 8 mm thickness Q460GJ steel plate, there were 56
141 specimens totally (2 specimens for each temperature 300, 400, 500, 600, 700, 800 and
142 900 °C and each pre-tensile stress 0, 0.3, 0.55 and 0.8). Similarly, for 12 mm thickness
143 Q460GJ steel plate, there were 56 specimens totally. The maximum test force of the
144 electronic high temperature tension measurement (GWT 2105) is 100 kN and the
145 relative error of test force indication is $\leq 0.5\%$. The high-temperature furnace was a
146 split type atmospheric furnace. The operating temperature ranges from 200 °C to 1100
147 °C and the temperature fluctuation was within 3 °C.

Table 2 Numbers of test specimens and corresponding test conditions.

Test number	T (°C)	$f_{y,T}$ (MPa)	Pre-tensile stress σ (MPa)	Stress ratio γ
GJ-8-300	300	411.86	0/123.6/226.5/329.5	0/0.3/0.55/0.8
GJ -8-400	400	375.82	0/112.7/206.7/300.7	0/0.3/0.55/0.8
GJ -8-500	500	311.94	0/93.6/171.6/249.5	0/0.3/0.55/0.8
GJ -8-600	600	220.42	0/66.1/121.2/176.3	0/0.3/0.55/0.8
GJ -8-700	700	108.74	0/32.6/59.8/87.0	0/0.3/0.55/0.8
GJ -8-800	800	53.78	0/16.1/29.6/43.0	0/0.3/0.55/0.8
GJ -8-900	900	38.43	0/11.5/21.1/30.7	0/0.3/0.55/0.8
GJ -12-300	300	443.13	0/132.9/243.7/354.5	0/0.3/0.55/0.8
GJ -12-400	400	415.55	0/124.5/228.25/332.4	0/0.3/0.55/0.8
GJ -12-500	500	365.29	0/109.6/200.9/292.2	0/0.3/0.55/0.8
GJ -12-600	600	249.76	0/74.9/137.4/199.8	0/0.3/0.55/0.8
GJ -12-700	700	120.18	0/36.1/66.1/96.1	0/0.3/0.55/0.8
GJ -12-800	800	54.44	0/16.3/29.9/43.6	0/0.3/0.55/0.8
GJ -12-900	900	35.38	0/10.6/19.5/28.3	0/0.3/0.55/0.8

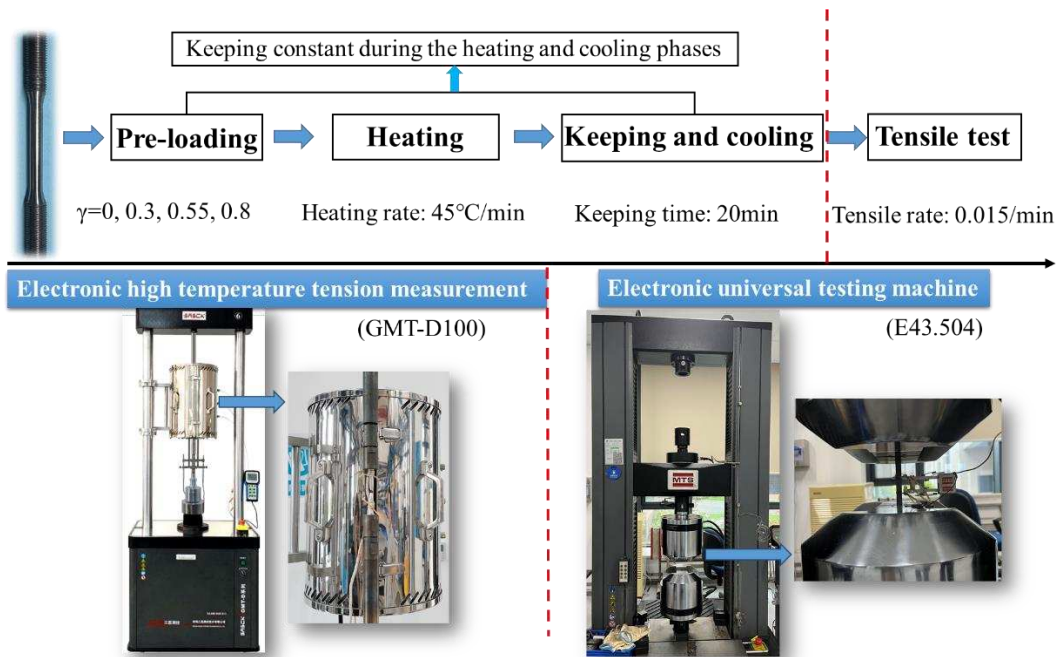


Fig. 2. Post-fire residual mechanical properties test procedure.

151 3.3 Tensile testing setup

152 The tensile test after heating at elevated temperature was carried out using the
153 electronic universal testing machine (E43.504) as shown in Figure 2. The maximum
154 load force of the electronic universal testing machine (E43.504) is 50 kN, and the
155 controllable test speed is 500 mm/min~0.001 mm/min. The displacement extensometer
156 was a ceramic rod extensometer, model 3448-025M-050, with a gauge length of 25.00
157 mm and a measurement accuracy of 0.001 mm. The loading system could apply
158 constant stress through servo motor and driver (Test force control stability $\pm 0.2\%$) to
159 ensure stress stability during the testing process. The numbers of test specimens and
160 corresponding test conditions are shown in Table 2. For example, the specimen number
161 ‘GJ-8-300-0.3-1’ represents ‘Q460GJ steel - 8mm thickness plate - 300 °C - pre-tensile
162 stress ratio 0.3 - specimen 1’. Two specimens were tested for each tensile test to ensure
163 the reliability of the test results and the two tested yield strength (f_{yT}) values were used
164 for error estimations. If the error exceeds 5%, the third one was tested, using the average
165 of the two acceptable test results as the representative value [33].

166 According to the stress-strain curve determined, four mechanical properties
167 including yield strength, ultimate strength, elastic modulus and apparent fracture
168 elongation were investigated. The elastic modulus was calculated by the slope of the
169 elastic section of the stress-strain curve. The yield strength was the lower boundary of
170 the yield platform. The ultimate strength was taken as the maximum value in the stress-
171 strain curve. The elongation after fracture was measured according to the provisions of
172 the standard GB/T 228.1 – 2010 (Tensile testing of metallic materials. Part 1: Room

173 temperature test method)[41]. The specific method was to firmly stick the fractured
174 parts of the specimen together, ensure that its axis was in the same straight line, and test
175 the gauge distance of the broken sample. The accuracy of vernier caliper used in
176 measurement was 0.01 mm, and the measurement error of elongation was 0.01%. The
177 elongation after fracture is obtained by the following equation (1):

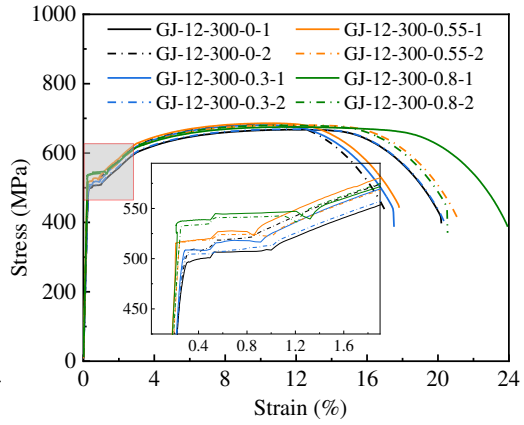
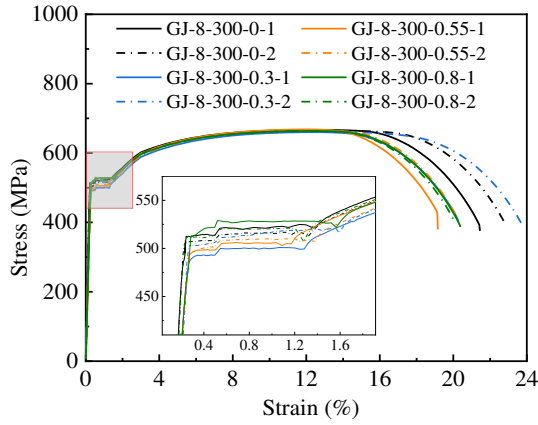
$$178 \quad \varepsilon = (L_u - L_0)/L_0 \times 100 \quad (1)$$

179 where ε is fracture elongation strain (%), L_u is the gauge length after fracture (mm), L_0
180 is the gauge length (40 mm).

181 **4. Post-fire tensile test results and discussions**

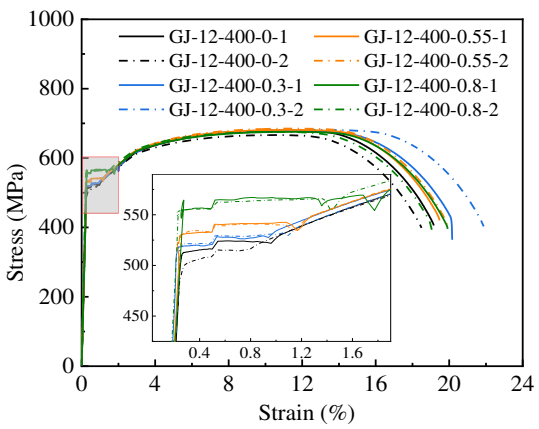
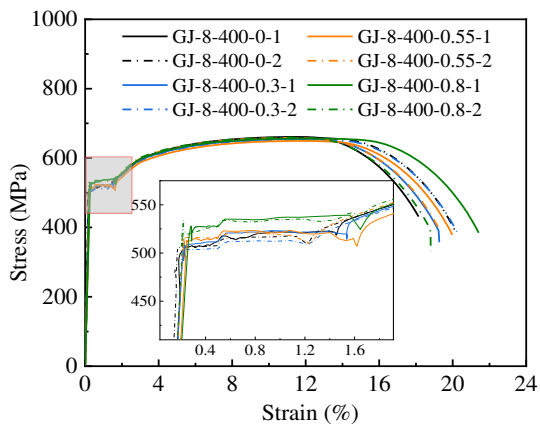
182 **4.1 Stress–strain (σ - ε) curves**

183 The stress-strain curves of Q460GJ steel after different elevated temperatures
184 heating are analyzed in the following. Figure 3 shows the post-fire tensile σ - ε curves of
185 Q460GJ steel specimens. The results of two test specimens in each test group were
186 similar after all temperatures heating. The pre-tensile stresses had no obvious effects on
187 the stress-strain curves of Q460GJ steel plate specimens. Only when the pre-tensile
188 stress ratio was 0.8, the yield strengths of the tested specimens were a little bite higher
189 than the others.



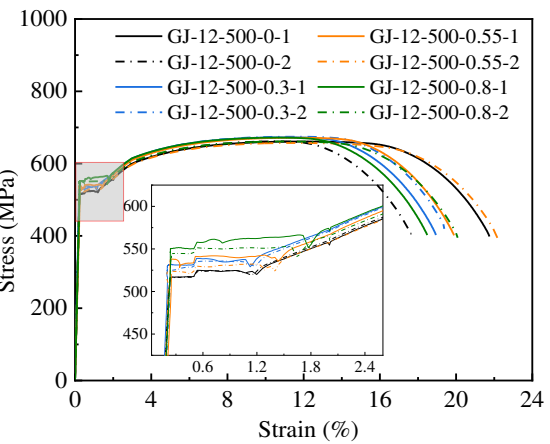
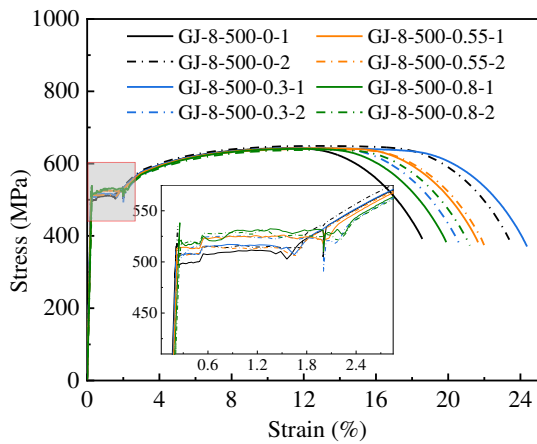
190

191 (a) GJ-8-300 specimens after 300 °C heating. (b) GJ-12-300 specimens after 300 °C heating.



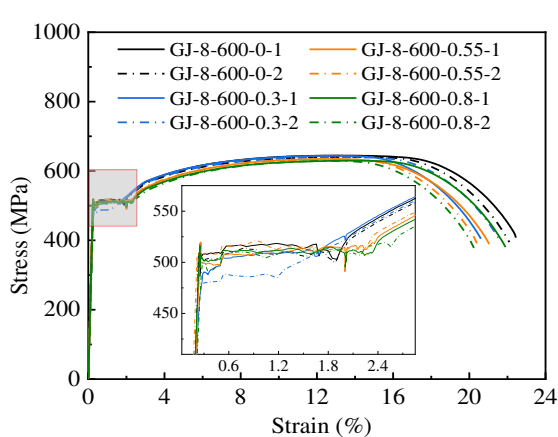
192

193 (c) GJ-8-400 specimens after 400 °C heating. (d) GJ-12-400 specimens after 400 °C heating.

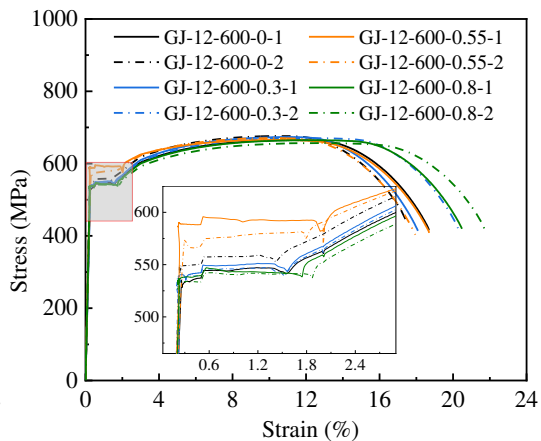


194

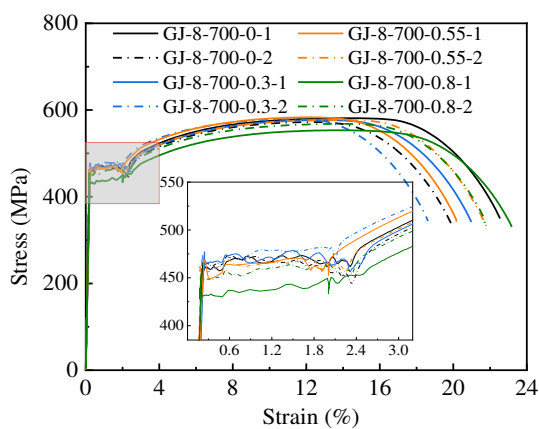
195 (e) GJ-8-500 specimens after 500 °C heating. (f) GJ-12-500 specimens after 500 °C heating.



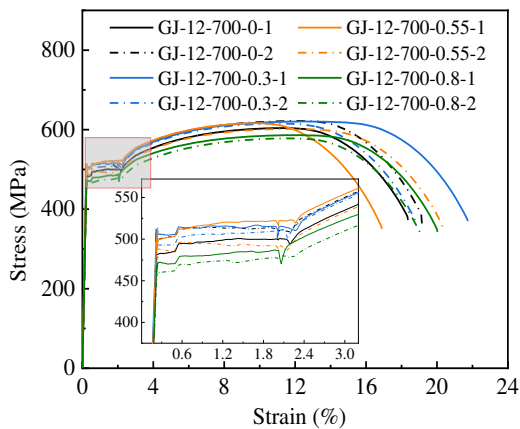
196



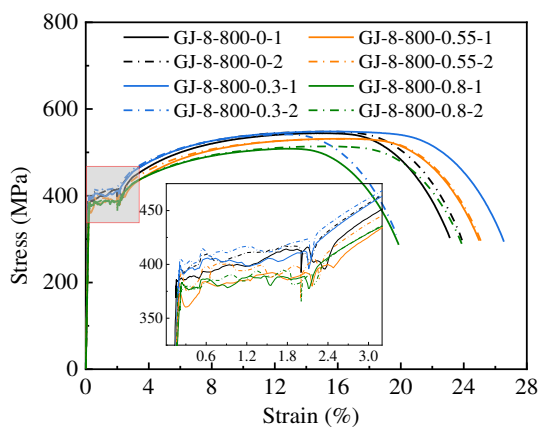
197 (g) GJ-8-600 specimens after 600 °C heating. (h) GJ-12-600 specimens after 600 °C heating.



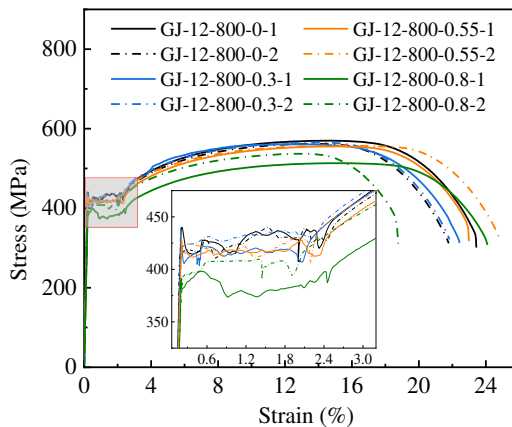
198



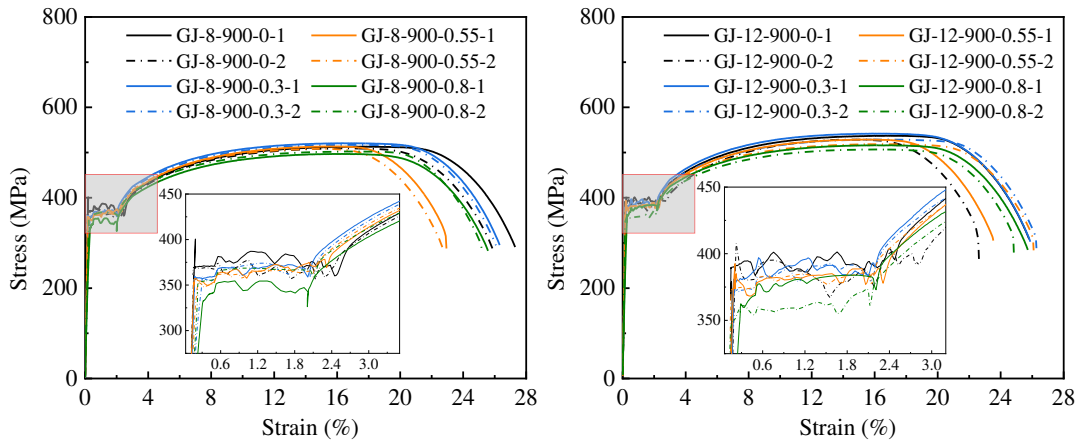
199 (i) GJ-8-700 specimens after 700 °C heating. (j) GJ-12-700 specimens after 700 °C heating.



200



201 (k) GJ-8-800 specimens after 800 °C heating. (l) GJ-12-800 specimens after 800 °C heating.



202

203 (m) GJ-8-900 specimens after 900 °C heating. (n) GJ-12-900 specimens after 900 °C heating.

204

Fig. 3. Post-fire tensile σ - ε curves of Q460GJ steel specimens.

205

206

207

208

209

210

211

212

213

214

215

216

The stress-strain curves of all the specimens showed a relatively obvious yield stage, and the heating temperature has little effect on the trend of the stress-strain curves of the tested specimens. When the heating temperatures were lower than 700 °C, the stress-strain curves were basically not affected by the heating temperatures. When the heating temperatures exceeded 700 °C, the ultimate stresses decreased significantly with the increase of temperature, while the deformation capacity increased. That the stress-strain curves of two types of Q460GJ steel plates with different thicknesses at all testing conditions were quite similar. The pre-tensile stresses had no obvious effects on the stress-strain curves of Q460GJ steel plate specimens, except for when the pre-tensile stress ratio was 0.8. The residual elastic modulus, yield strength, ultimate strength and fracture elongation of Q460GJ steel after different elevated temperatures heating are analyzed in the following.

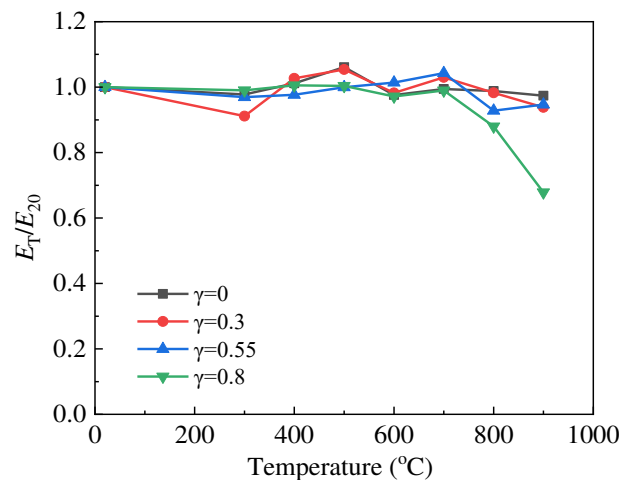
217

4.2 Elastic modulus (E_T) reduction factor

218

The elastic modulus (E_T) average was calculated based on the tested average

219 results of 8 mm thickness Q460GJ steel plate and 12 mm thickness Q460GJ steel plate.
 220 Table 3 shows the post-fire elastic modulus reduction factors (E_T/E_{20}) with different
 221 pre-tensile ratios. The elastic modulus of Q460GJ steel plates were cited from the
 222 reference [43] as 230.490 GPa for 8 mm thickness Q460GJ steel plate and 205.180 GPa
 223 for 12 mm thickness Q460GJ steel plate. Then the post-fire elastic modulus reduction
 224 factors (E_T/E_{20}) of Q460GJ steel plates specimens were calculated and shown in Figure
 225 4. It can be found that the elastic modulus of the two kinds of Q460GJ steel plates after
 226 elevated temperature heating remained relatively unchanged below 800 °C, and the
 227 fluctuation range was within 10%. While the elevated temperature was 400 °C and pre-
 228 tensile ratio was 0.3, the reduction coefficient was a little bit higher, this might be
 229 caused by experimental error. When the elevated temperature reached 900 °C, the elastic
 230 modulus decreased slightly when the applied stress ratio is within 0.55, but it decreased
 231 by about 30% when the stress ratio was 0.8. This indicates that the Q460GJ steel will
 232 lose part of its stiffness when exposed to 20 min 900 °C elevated temperature and with
 233 a high pre-tensile stress ratio at the same time.



234

235

Fig. 4. The post-fire elastic modulus reduction factors (E_T/E_{20}) of Q460GJ steel plates.

236 Table 3 The post-fire elastic modulus reduction factors (E_T/E_{20}) with different pre-tensile ratios.

Steel plates number	E_T/E_{20}			
	$\gamma = 0$	$\gamma = 0.3$	$\gamma = 0.55$	$\gamma = 0.8$
GJ-20	1.000	-	-	-
GJ-300	0.977	0.912	0.970	0.990
GJ-400	1.012	1.027	0.977	1.005
GJ-500	1.061	1.054	1.000	1.004
GJ-600	0.976	0.982	1.014	0.972
GJ-700	0.994	1.030	1.043	0.990
GJ-800	0.988	0.983	0.928	0.880
GJ-900	0.974	0.938	0.947	0.678

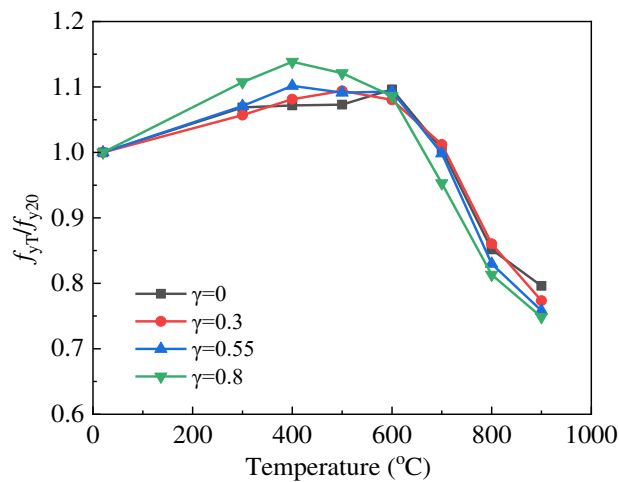
237 **4.3 Yield strength (f_{yT}) reduction factor**

238 The yield strength (f_{yT}) average was calculated based on the tested average results
 239 of 8 mm thickness Q460GJ steel plate and 12 mm thickness Q460GJ steel plate. Table
 240 4 shows the post-fire yield strength reduction factors with different pre-tensile ratios.
 241 The yield strengths (f_{y20}) of Q460GJ steel plates were cited from the reference [43] as
 242 475.6 MPa for 8 mm thickness Q460GJ steel plate and 495.7 MPa for 12 mm thickness
 243 Q460GJ steel plate. Then the post-fire yield strength reduction factors (f_{yT}/f_{y20}) of
 244 Q460GJ steel plates specimens were calculated and shown in Figure 5. It can be found
 245 that the yield strengths of the two kinds of Q460GJ steel plates after elevated
 246 temperature heating remained relatively unchanged below 700 °C. When the elevated
 247 temperature reached 700 °C, the yield strength decreased significantly by more than
 248 20%. The yield strength degraded seriously when exposed to 900 °C elevated
 249 temperature. By comparing the yield strengths with different pre-tensile stress ratios, it

250 was found that when the heating elevated temperatures were 600 °C and below, the pre-
 251 tensile stress ratio has little effect on the yield strength. When the heating elevated
 252 temperatures were above 700 °C, the yield strength decreased gradually with the
 253 increase of pre-tensile stress ratio, especially when the pre-tensile stress ratios were
 254 above 0.55.

255 Table 4 The post-fire yield strength reduction factors with different pre-tensile ratios.

Steel plates number	f_{yT}/f_{y20}			
	$\gamma = 0$	$\gamma = 0.3$	$\gamma = 0.55$	$\gamma = 0.8$
GJ-20	1.000	-	-	-
GJ-300	1.069	1.057	1.071	1.107
GJ-400	1.072	1.081	1.102	1.138
GJ-500	1.073	1.094	1.091	1.121
GJ-600	1.096	1.080	1.093	1.086
GJ-700	1.005	1.012	0.999	0.953
GJ-800	0.852	0.860	0.830	0.813
GJ-900	0.796	0.774	0.758	0.749



256

257 Fig. 5. The post-fire yield strength reduction factors (f_{yT}/f_{y20}) of Q460GJ steel plates.

258 The yield strength increased slightly when the heating elevated temperatures were

259 within 300 °C to 600 °C, which might be due to the change of microstructure of Q460GJ
260 steel caused by elevated temperature heating and cooling. Based on this study, the yield
261 strength of Q460GJ steel did not lose when the heating elevated temperature was below
262 700 °C and the applied pre-tensile stress ratio was within 0.8. It may be concluded that,
263 if Q460GJ steel member is exposed to fire temperature below 700 °C for no more than
264 20 minutes, it can be reused after fire.

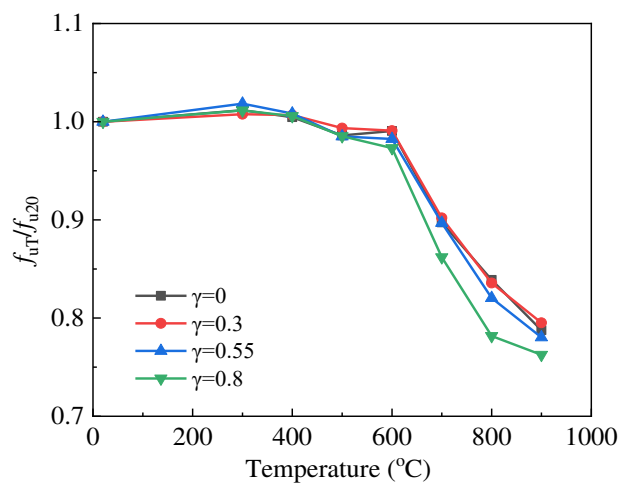
265 **4.4 Ultimate strength (f_{uT}) reduction factor**

266 The ultimate strength (f_{uT}) average was calculated based on the tested average
267 results of 8 mm thickness Q460GJ steel plate and 12 mm thickness Q460GJ steel plate.
268 Table 5 shows the post-fire ultimate strength reduction factors with different pre-tensile
269 ratios. The ultimate strengths (f_{u20}) of Q460GJ steel plates were cited from the reference
270 [43] as 663 MPa for 8 mm thickness Q460GJ steel plate and 681.1 MPa for 12 mm
271 thickness Q460GJ steel plate. Then the post-fire ultimate strength reduction factors ($f_{uT}/$
272 f_{u20}) of Q460GJ steel plates specimens were calculated and shown in Figure 6. It can be
273 found that the ultimate strengths of the two kinds of Q460GJ steel plates after elevated
274 temperature heating remained relatively unchanged below 600 °C. When the elevated
275 temperature reached 800 °C, the ultimate strength decreased significantly by more than
276 10%. The ultimate strength of Q460GJ steel degraded seriously when exposed to 900
277 °C elevated temperature. By comparing the ultimate strengths with different pre-tensile
278 stress ratios, it was found that when the heating elevated temperatures were 600 °C and
279 below, the pre-tensile stress ratio has little effect on the ultimate strength. When the

280 heating elevated temperatures were above 600 °C, the ultimate strength decreased
 281 gradually with the increase of pre-tensile stress ratio, especially when the pre-tensile
 282 stress ratios were above 0.55. The change trend of ultimate strength after elevated
 283 temperature heating and cooling was consistent with that of yield strength for Q460GJ
 284 steel.

285 Table 5 The post-fire ultimate strength reduction factors with different pre-tensile ratios.

Steel plates number	f_{uT}/f_{u20}			
	$\gamma = 0$	$\gamma = 0.3$	$\gamma = 0.55$	$\gamma = 0.8$
GJ-20	1.000	-	-	-
GJ-300	1.012	1.008	1.018	1.012
GJ-400	1.005	1.007	1.008	1.006
GJ-500	0.986	0.993	0.985	0.985
GJ-600	0.991	0.991	0.982	0.973
GJ-700	0.897	0.902	0.897	0.862
GJ-800	0.839	0.836	0.820	0.782
GJ-900	0.788	0.795	0.780	0.763

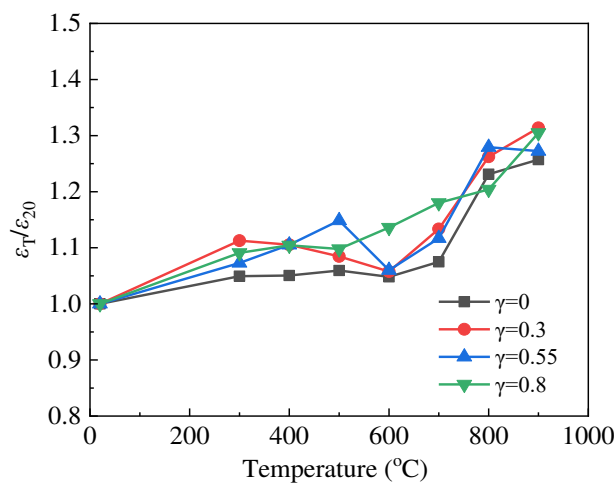


286

287 Fig. 6. The post-fire ultimate strength reduction factors (f_{uT}/f_{u20}) of Q460GJ steel plates.

288 **4.5 Ultimate elongation (ϵ_T) reduction factor**

289 The ultimate elongation (ϵ_T) average was calculated based on the tested average
290 results of 8 mm thickness Q460GJ steel plate and 12 mm thickness Q460GJ steel plate.
291 Table 6 shows the of post-fire ultimate elongation reduction factors with different pre-
292 tensile ratios. The ultimate elongations (ϵ_{20}) of Q460GJ steel plates were cited from the
293 reference [43] as 26.76% for 8 mm thickness Q460GJ steel plate and 23.94% for 12
294 mm thickness Q460GJ steel plate. Then the post-fire ultimate elongation reduction
295 factors ($\epsilon_T / \epsilon_{20}$) of Q460GJ steel plates specimens were calculated and shown in Figure
296 7. The ultimate elongation increased with the increase of heating temperature. By
297 comparing the ultimate elongations with different pre-tensile stress ratios, it was found
298 that pre-tensile stress ratio did not have obvious effect on the ultimate elongation. The
299 specimens after elevated temperature heating and cooling showed higher ductility than
300 those without elevated temperature heating and cooling. Q460GJ steel still maintains
301 good ductility after elevated temperature heating, which increases the possibility of
302 reuse of Q460GJ steel element after fire.



303

304 Fig. 7. The post-fire ultimate strength reduction factors ($\epsilon_T / \epsilon_{20}$) of Q460GJ steel plates.

305 Table 6 The of post-fire ultimate elongation reduction factors with different pre-tensile ratios.

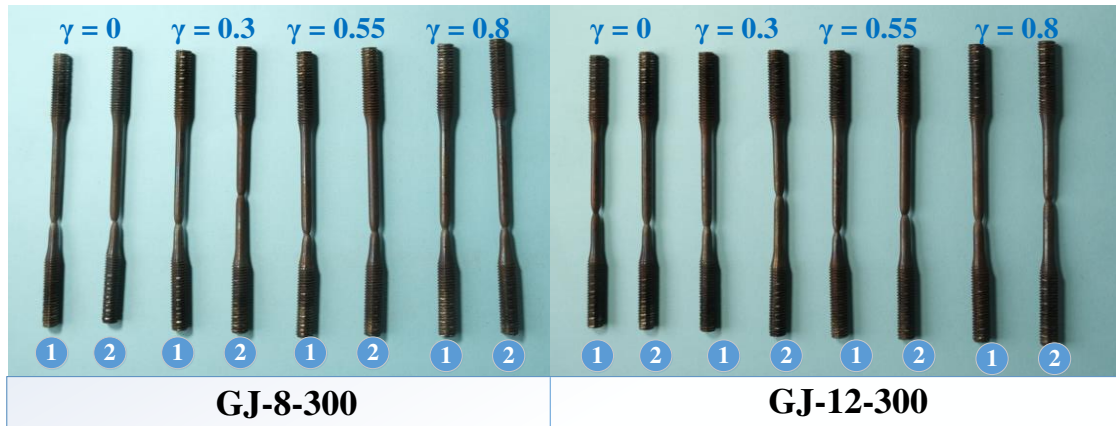
Steel plates number	$\varepsilon_T/\varepsilon_{20}$			
	$\gamma = 0$	$\gamma = 0.3$	$\gamma = 0.55$	$\gamma = 0.8$
GJ-20	1.000	-	-	-
GJ-300	1.049	1.113	1.073	1.091
GJ-400	1.051	1.106	1.105	1.104
GJ-500	1.059	1.085	1.149	1.098
GJ-600	1.048	1.058	1.060	1.136
GJ-700	1.075	1.134	1.117	1.180
GJ-800	1.231	1.262	1.279	1.204
GJ-900	1.257	1.314	1.272	1.305

306

307 4.6 Apparent failure modes

308 Figure 8 shows the apparent failure modes of the tensile specimens after elevated
 309 temperature heating and cooling. The typical fracture site side view photos of
 310 specimens after testing are shown in Figure 9. It can be seen that each specimen
 311 exhibited ductile and necking failure. With the increase of the heating elevated
 312 temperature, the length of the Q460GJ steel specimen at failure increased, so the
 313 ductility was better. It can be seen from the photos that the apparent color of the
 314 specimens gradually turns black with the increase of the heating temperature, indicating
 315 that the oxidation degree gradually increases. With 400 °C heating elevated temperature,
 316 the blue brittleness phenomenon was observed. With higher heating elevated
 317 temperature, the oxidation on the surface of the steel specimen is more severe. This
 318 causes the different color of the specimen surfaces formed at heating elevated
 319 temperatures. This surface color changing could be potentially used as a useful indicator

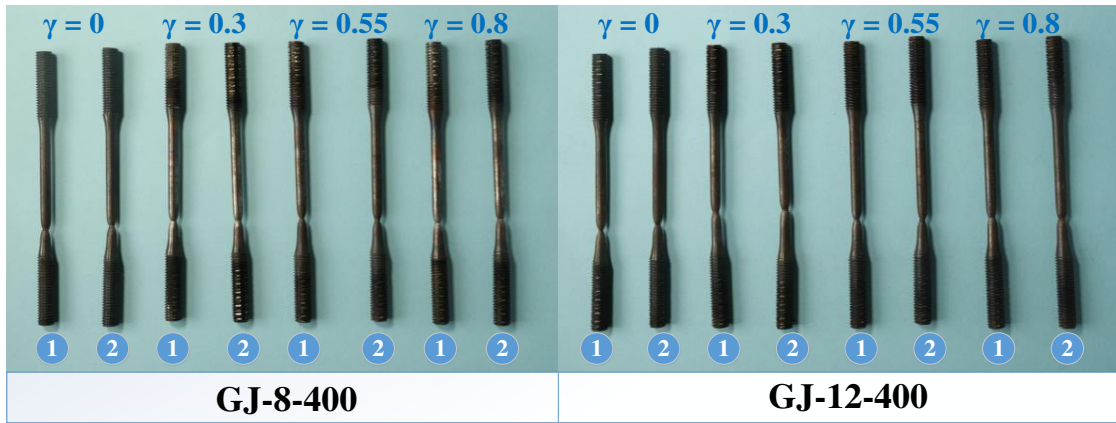
320 of fire temperature.



321

322

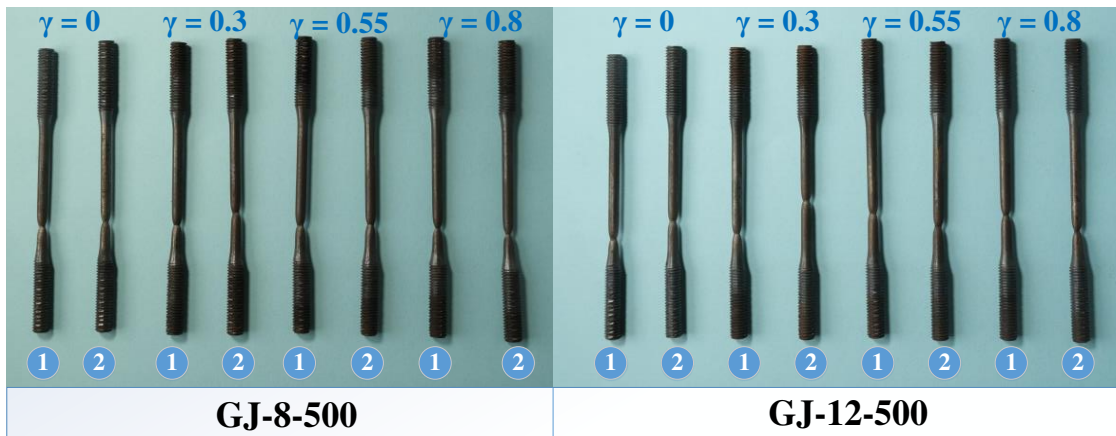
(a) After 20 min 300 °C heating.



323

324

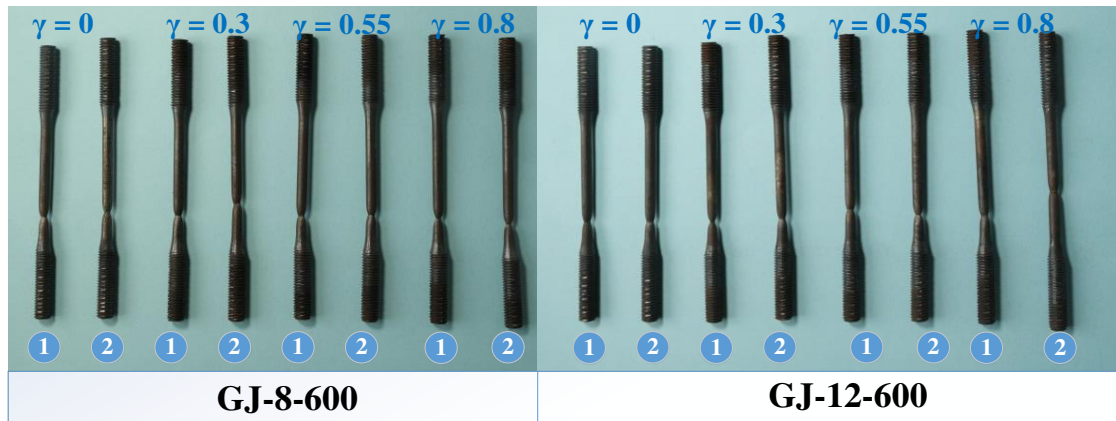
(b) After 20 min 400 °C heating.



325

326

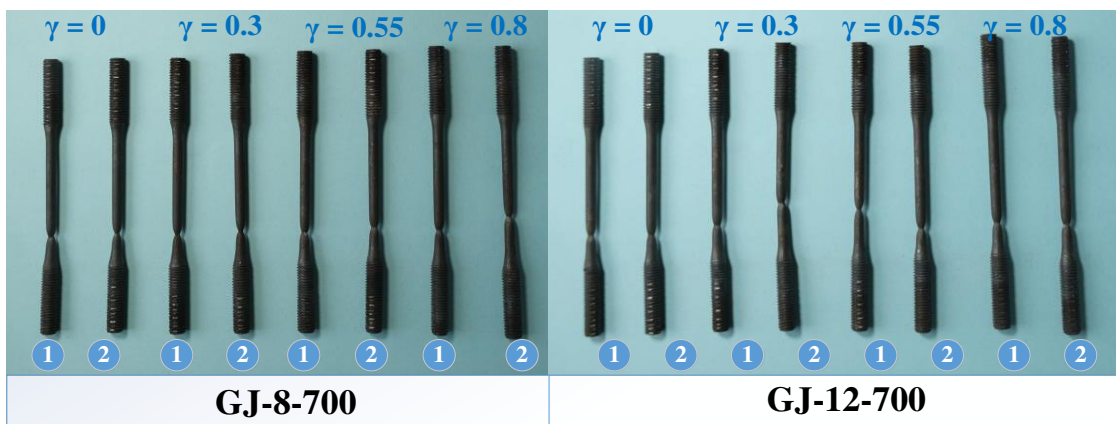
(c) After 20 min 500 °C heating.



327

328

(d) After 20 min 600 °C heating.



329

330

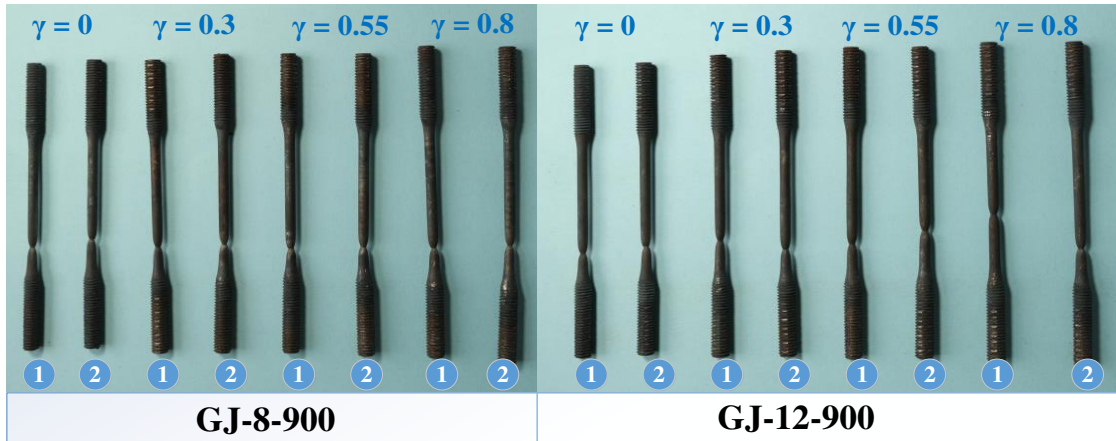
(e) After 20 min 700 °C heating.



331

332

(f) After 20 min 800 °C heating.



(g) After 20 min 900 °C heating.

Fig. 8. Apparent failure modes of specimens after testing.

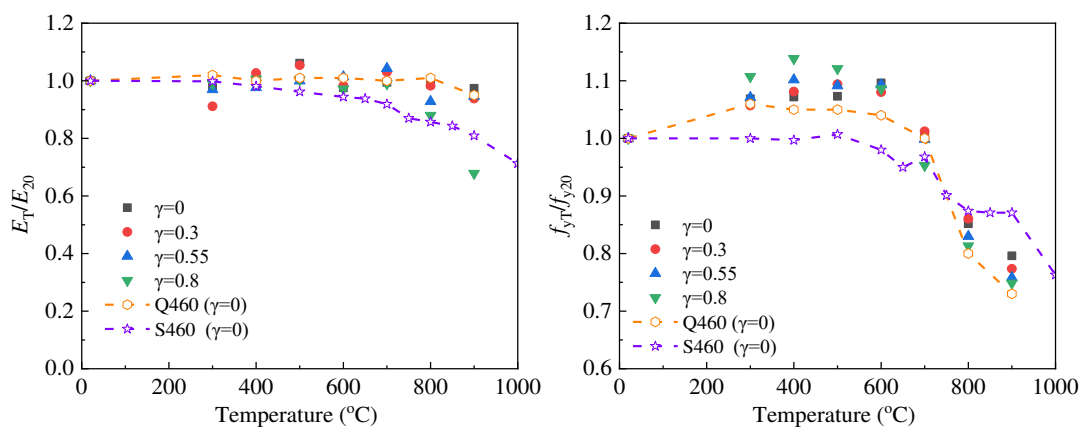


Fig. 9. Typical fracture site side view photos of specimens after testing.

5. Comparison with Q460 and S460 steels

Because the chemical composition and microstructure of different steels are different, the heating temperature and cooling mode may have different effects on the mechanical properties of different steels after heating and cooling. Figure 10 shows the comparison of the post-fire residual mechanical properties of Q460GJ steel and referred Q460 [31] and S460 [28] steels. The elastic modulus reduction factors are shown in Figure 10 (a). It can be found that Q460GJ steel had the same trend as Q460 and S460

345 steels, which was basically not affected by the heating elevated temperature, except for
 346 above 800 °C, the elastic modulus reduction factors decreased significantly. The yield
 347 strength reduction factors are shown in Figure 10 (b). It can be found that Q460GJ steel
 348 had the same trend of yield strength reduction factor as Q460 steel. The yield strength
 349 reduction factors of Q460 steel after elevated temperature heating and cooling were
 350 higher than that of S460 steel when the heating temperatures were within 700 °C, and
 351 lower than that of S460 steel when the heating temperatures were above 700 °C. The
 352 ultimate strength reduction factors are shown in Figure 10 (c). It can be found that We
 353 found that Q460GJ steel and Q460 and S460 steels had similar overall trends. However,
 354 when the heating temperatures were above 700 °C, the yield strength reduction factors
 355 of Q460GJ steel after elevated temperature heating and cooling were obviously lower
 356 than that of Q460 and S460 steels. The ultimate elongation reduction factors are shown
 357 in Figure 10 (d). On the whole, the ultimate elongation reduction factors of Q460GJ
 358 steel after elevated temperature heating and cooling were greater than that of Q460 steel.
 359 Especially within 700 °C, the ultimate elongation reduction factors of Q460 steel were
 360 all less than 1.0. Therefore, to sum up, Q460GJ steel has better ductility after elevated
 361 temperature heating and cooling than that of Q460 steel.

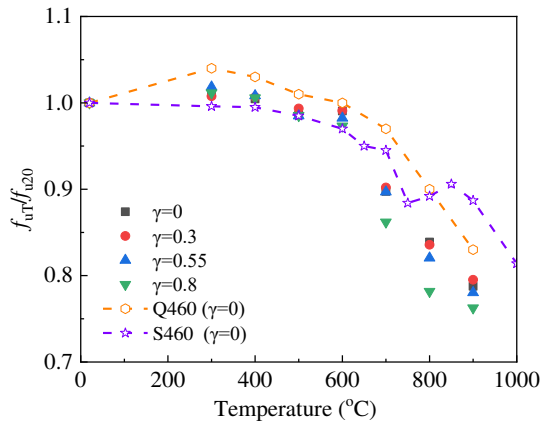


362

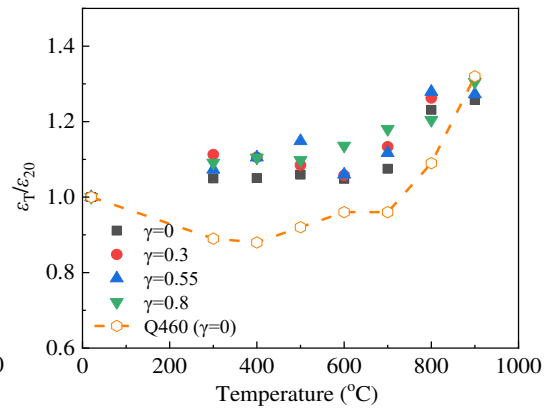
363

(a) Elastic modulus reduction factors.

(b) Yield strength reduction factors.



364



365

(c) Ultimate strength reduction factors.

(d) Ultimate elongation reduction factors.

366

Fig. 10. Comparison of Q460GJ steel and referred Q460 and S460 steels.

367

6. Predictive equations for residual mechanical properties

368

369 Based on the above experimental results, it can be found that the residual
 370 mechanical properties of Q460GJ steel after elevated temperature heating and cooling
 371 were different with that of Q460 steel and S460 steel. It is necessary to establish the
 372 predictive equations for the residual mechanical properties for Q460GJ steel after
 373 elevated temperature heating and cooling under different pre-tensile stresses. The tested
 374 results also showed that the effect of plate thickness on the mechanical properties of
 375 Q460GJ steel could be ignored. Therefore, a set of unified prediction equations for the
 376 reduction factors of mechanical properties of two kinds of plate thickness are proposed
 as the followings.

377

6.1 Elastic modulus reduction factor

378

Experimental results in section 4.2 showed that the elastic modulus of Q460GJ

379 steel had little change after elevated temperature heating and cooling, and it was
 380 reduced only at the pre-tensile stress ratio of 0.8. Therefore, in this paper the predictive
 381 equation of the elastic modulus reduction factors after elevated temperatures heating
 382 and cooling under the stress ratio of 0.8 was proposed only, and the predictive equation
 383 was shown as equation (2) and the predictive equation fitting with experimental results
 384 was shown in Figure 11(a).

$$385 \quad E_T/E_{20} = \begin{cases} 1 & 20^\circ\text{C} \leq T_s \leq 900^\circ\text{C}, \gamma = 0/0.3/0.55 \\ -2.571 \times 10^{-9} T_s^3 + 2.704 \times 10^{-6} T_s^2 - 7.111 \times 10^{-4} T_s + 1.016 & 20^\circ\text{C} \leq T_s \leq 900^\circ\text{C}, \gamma = 0.8 \end{cases} \quad (2)$$

386 6.2 Yield strength reduction factor

387 The tested results in section 4.3 show that although the yield strength of Q460GJ
 388 steel after elevated temperature heating and cooling had little change when the elevated
 389 temperatures were within 700 °C, the yield strength of Q460GJ steel had a significant
 390 reduction above 700 °C, and the reduction degree of yield strength was different under
 391 different pre-tensile stress ratios. The predictive equation of the yield strength reduction
 392 factors after elevated temperatures heating and cooling under different pre-tensile stress
 393 ratios was proposed, and the predictive equation was shown as equation (3) and the
 394 predictive equation fitting with experimental results was shown in Figure 11(b).

$$395 \quad f_{yT}/f_{y20} = \begin{cases} -1.044 \times 10^{-9} T_s^3 + 4.097 \times 10^{-7} T_s^2 + 2.308 T_s + 0.993 & 20^\circ\text{C} \leq T_s \leq 900^\circ\text{C}, \gamma = 0 \\ -1.371 \times 10^{-9} T_s^3 + 7.920 \times 10^{-7} T_s^2 + 1.304 T_s + 0.994 & 20^\circ\text{C} \leq T_s \leq 900^\circ\text{C}, \gamma = 0.3 \\ -1.066 \times 10^{-9} T_s^3 + 2.620 \times 10^{-7} T_s^2 + 3.418 T_s + 0.989 & 20^\circ\text{C} \leq T_s \leq 900^\circ\text{C}, \gamma = 0.55 \\ 4.658 \times 10^{-12} T_s^3 - 1.356 \times 10^{-6} T_s^2 + 9.341 T_s + 0.976 & 20^\circ\text{C} \leq T_s \leq 900^\circ\text{C}, \gamma = 0.8 \end{cases} \quad (3)$$

396 6.3 Ultimate strength reduction factor

397 The tested results in section 4.4 show that although the ultimate strength of

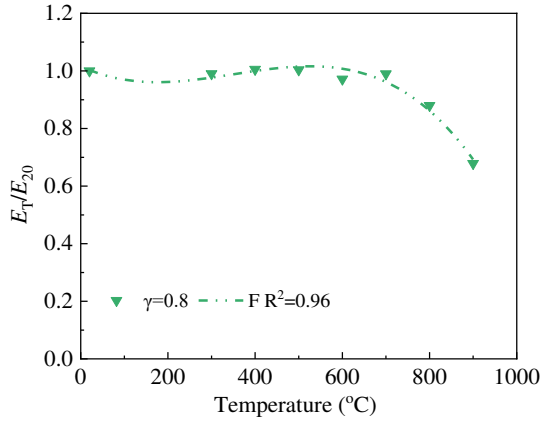
398 Q460GJ steel after elevated temperature heating and cooling had little change when the
399 elevated temperatures were within 700 °C, the ultimate strength of Q460GJ steel had a
400 significant reduction above 700 °C, and the reduction degree of ultimate strength was
401 different under different pre-tensile stress ratios. The predictive equation of the ultimate
402 strength reduction factors after elevated temperatures heating and cooling under
403 different pre-tensile stress ratios was proposed, and the predictive equation was shown
404 as equation (4) and the predictive equation fitting with experimental results was shown
405 in Figure 11(c).

$$406 \quad f_{ut}/f_{u20} = \begin{cases} -2.609 \times 10^{-10} T_s^3 - 2.091 \times 10^{-7} T_s^2 + 1.576 \times 10^{-4} T_s + 0.995 & 20^\circ\text{C} \leq T_s \leq 900^\circ\text{C}, \gamma = 0 \\ -2.594 \times 10^{-10} T_s^3 - 2.091 \times 10^{-7} T_s^2 + 1.620 \times 10^{-4} T_s + 0.995 & 20^\circ\text{C} \leq T_s \leq 900^\circ\text{C}, \gamma = 0.3 \\ -8.686 \times 10^{-11} T_s^3 - 4.797 \times 10^{-7} T_s^2 + 2.516 \times 10^{-4} T_s + 0.994 & 20^\circ\text{C} \leq T_s \leq 900^\circ\text{C}, \gamma = 0.55 \\ 2.014 \times 10^{-10} T_s^3 - 9.086 \times 10^{-7} T_s^2 + 3.807 \times 10^{-4} T_s + 0.989 & 20^\circ\text{C} \leq T_s \leq 900^\circ\text{C}, \gamma = 0.8 \end{cases} \quad (4)$$

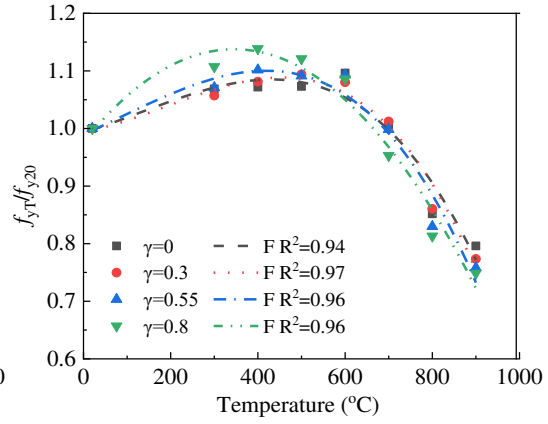
407 **6.4 Ultimate elongation reduction factor**

408 The predictive equation of the ultimate elongation reduction factors after elevated
409 temperatures heating and cooling under different pre-tensile stress ratios was proposed,
410 and the predictive equation was shown as equation (5) and the predictive equation
411 fitting with experimental results was shown in Figure 11(d). In this article, three main
412 pre-tensile stress ratios of 0.30, 0.55 and 0.80 were designed and the scope of tensile
413 stress ratios basically covers the actual engineering situation. Linear interpolation
414 method could be used to determine the retention of mechanical properties with other
415 stress ratios.

$$\begin{aligned}
416 \quad \varepsilon_T/\varepsilon_{20} = & \begin{cases} 1.387 \times 10^{-9} T_s^3 - 1.435 \times 10^{-6} T_s^2 + 4.869 \times 10^{-4} T_s + 0.992 & 20^\circ\text{C} \leq T_s \leq 900^\circ\text{C}, \gamma = 0 \\ 2.267 \times 10^{-9} T_s^3 - 2.714 \times 10^{-6} T_s^2 + 0.001 T_s + 0.984 & 20^\circ\text{C} \leq T_s \leq 900^\circ\text{C}, \gamma = 0.3 \\ 1.355 \times 10^{-9} T_s^3 - 1.604 \times 10^{-7} T_s^2 + 6.933 \times 10^{-4} T_s + 0.986 & 20^\circ\text{C} \leq T_s \leq 900^\circ\text{C}, \gamma = 0.55 \\ 1.138 \times 10^{-9} T_s^3 - 1.347 \times 10^{-6} T_s^2 + 6.374 \times 10^{-4} T_s + 0.988 & 20^\circ\text{C} \leq T_s \leq 900^\circ\text{C}, \gamma = 0.8 \end{cases} \quad (5)
\end{aligned}$$

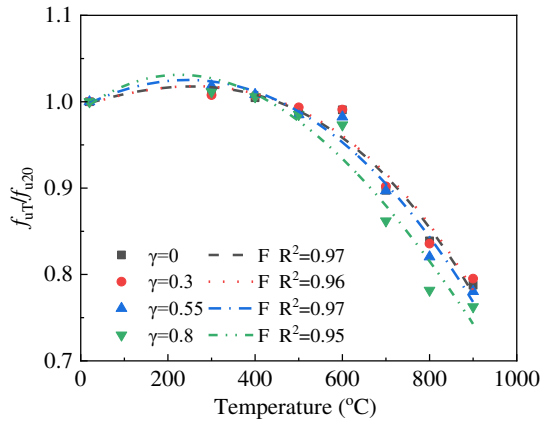


417

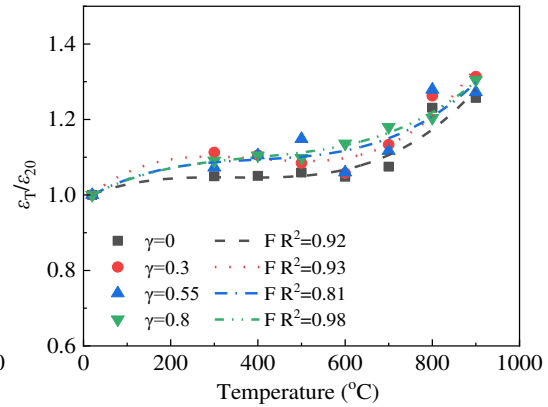


418 (a) Elastic modulus equation fitting.

(b) Yield strength equations fitting.



419



420 (c) Ultimate strength equations fitting.

(d) Ultimate elongation equations fitting.

421 Fig. 11. Fittings of the predictive equations for the residual mechanical properties.

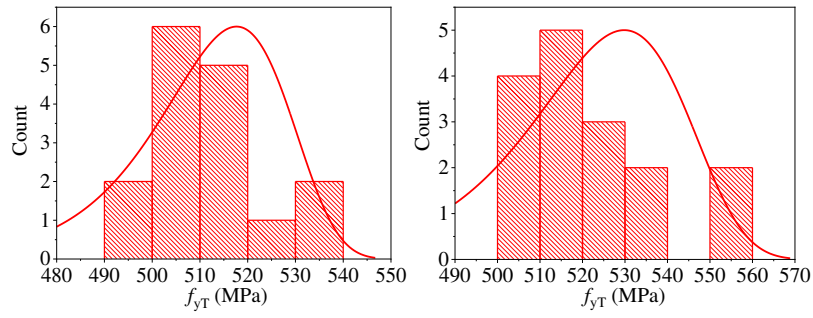
422 7. Variation coefficient of yield strength of Q460GJ steel

423 Since there are few references on the detailed specifications of mechanical
424 parameters at elevated temperatures for Q460GJ steel in current design specifications,
425 it is necessary to carry out a reliability analysis of yield strength of Q460GJ steel
426 obtained with the test results. The frequency distribution histograms of f_{yT} for Q460GJ

427 steels after 20 min different elevated temperatures heating are shown in Figure 12.
428 According to the AISI-S100 (2020) standard (Section K2.1.1) [44], the results of
429 statistical analysis of yield strength are shown in Table 7. Table 7 shows the standard
430 values of yield strength (f_{yT}) for the tested Q460GJ steel under different pre-tensile
431 stresses after 20 min different elevated temperatures heating, which is determined by
432 the 5% quantile of the Weibull's probability distribution. The standard value $\mu_{f_{yT}}$,
433 standard deviation $\sigma_{f_{yT}}$ and variation coefficient $\delta_{f_{yT}}$ of the yield strength for Q460GJ
434 steel are shown in Table 7, which shows that based on the current sample conditions,
435 the values of variation coefficient $\delta_{f_{yT}}$ are reasonable ranged from 0.032 to 0.051,
436 indicating that the standard values $\mu_{f_{yT}}$ can provide a reference for the further reliability
437 analysis of Q460GJ steel at the component level. The variation coefficient $\delta_{f_{yT}}$ of the
438 yield strength for Q460GJ steel at about 700 °C is slightly larger (0.051), mainly
439 because the mechanical properties of steel change rapidly at about 700 °C.

440 To sum up, the statistical analysis method (Weibull's probability distribution) was
441 used to study the uniformity for Q460GJ steel under different pre-tensile stresses after
442 different elevated temperatures heating. The results showed that the different pre-tensile
443 stresses and different elevated temperatures heating did not affect the uniformity of steel
444 yield strength. These experimental results demonstrate that uniform temperature and
445 stress changes do not affect the uniformity of the material commonly. The variation
446 coefficients $\delta_{f_{yT}}$ of the yield strength for Q460GJ steel under different pre-tensile
447 stresses after 20 min different elevated temperatures heating were within 0.065. The
448 experimental results provide scientific support for the re-use determination of under

449 different pre-tensile stresses after different elevated temperatures heating.

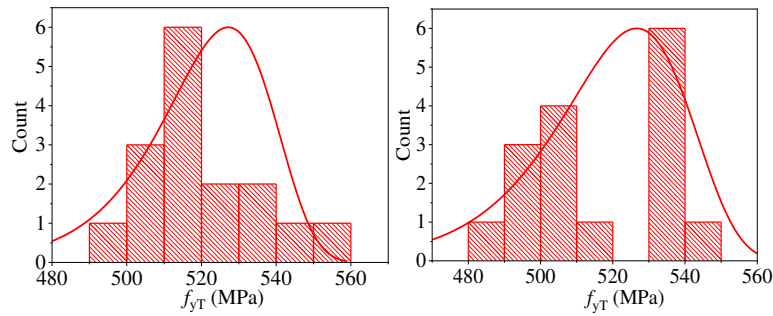


450

451

(a) After 20 min 300 °C heating.

(b) After 20 min 400 °C heating.

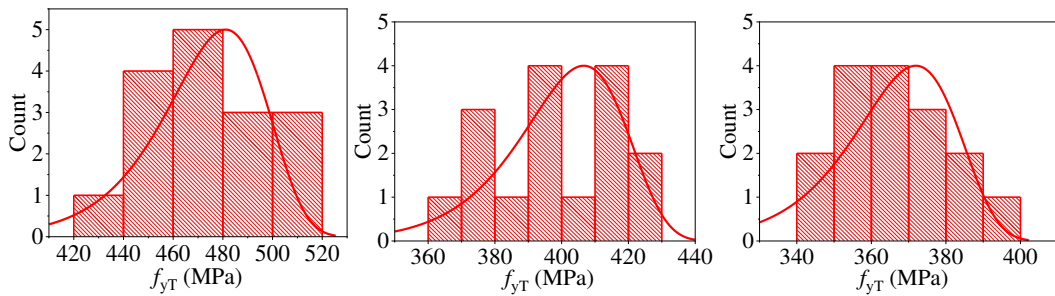


452

453

(c) After 20 min 500 °C heating.

(d) After 20 min 600 °C heating.



454

455

(e) After 20 min 700 °C heating. (f) After 20 min 800 °C heating. (g) After 20 min 900 °C heating.

456

Fig. 12. Frequency distribution histogram of f_{yT} for Q460GJ steel after 20 min heating.

457

Table 7 The results of statistical analysis of f_{yT} for Q460GJ steel after 20 min heating.

T (°C)	Statistical parameters		
	$\mu_{f_{yT}}$	$\sigma_{f_{yT}}$	$\delta_{f_{yT}}$
300	510.731	16.353	0.032
400	520.855	21.568	0.041
500	519.642	17.837	0.034
600	517.716	21.408	0.041
700	471.328	24.003	0.051
800	398.943	18.633	0.047
900	365.068	16.605	0.045

458

8. Conclusions

459

460

461

462

In this article, the post-fire residual mechanical properties of Q460GJ steel with two kinds of plate thickness (8 mm and 12 mm) under different pre-tensile stresses were studied. Based on the experimental results and calculation analyses, the following major findings are revealed.

463

464

465

466

467

468

(1) The stress-strain curves of two types of Q460GJ steel plates with different thicknesses at all testing conditions were quite similar. The difference in plate thickness does not affect the residual mechanical properties of the 8mm and 12mm Q460GJ steel plates. The pre-tensile stresses had no obvious effects on the stress-strain curves of Q460GJ steel plate specimens after 20 min elevated temperature heating, except for when the pre-tensile stress ratio was 0.8.

469

470

471

(2) The Q460GJ steel will lose part of its stiffness when exposed to 900 °C elevated temperature and with a high pre-tensile stress ratio at the same time. The yield strength of Q460GJ steel did not lose when the heating elevated temperature was below 700 °C

472 and the applied pre-tensile stress ratio was within 0.8. When the heating elevated
473 temperatures were 600 °C and below, the pre-tensile stress ratio has little effect on the
474 yield strength. When the heating elevated temperatures were above 600 °C, the ultimate
475 strength decreased gradually with the increase of pre-tensile stress ratio, especially
476 when the pre-tensile stress ratios were above 0.55. Q460GJ steel still maintains good
477 ductility after elevated temperature heating, which increases the possibility of reuse of
478 Q460GJ steel element after fire.

479 (3) The residual mechanical properties of Q460GJ steel after elevated temperature
480 heating and cooling were different with that of Q460 steel and S460 steel. The Q460GJ
481 steel has better ductility after elevated temperature heating and cooling than that of
482 Q460 and S460 steels.

483 (4) The predictive equations for the residual mechanical properties for Q460GJ
484 steel after elevated temperature heating and cooling under different pre-tensile stresses
485 were proposed and were in good agreement with the experimental results of this study.
486 The different pre-tensile stresses and different elevated temperatures heating did not
487 affect the uniformity of steel yield strength. The findings should have a great
488 significance to providing theoretical support for design of reusing or restoring the steel
489 building after fire.

490 **Acknowledgment**

491 The authors wish to acknowledge the support of the Fundamental Research Funds
492 for the Central Universities (Grant No.: 2023CDJKYJH018), the Natural Science

493 Foundation of Chongqing (Grant No.: cstc2021jcyj-jqX0021), and Hegang
494 Construction Engineering Co., Ltd (Grant No.: H20221023). Any opinions, findings,
495 conclusions, or recommendations expressed in this paper are those of the authors and
496 do not necessarily reflect the views of the sponsors.

497 **References**

- 498 [1] Xing Y, Zhao O, Wang W. Testing, modelling and analysis of full-scale cold-formed steel
499 center-sheathed shear walls in fire [J]. *Engineering Structures*, 2023, 284: 115970
- 500 [2] Zhai S Y, Lyu Y F, Cao K, et al. Seismic behavior of an innovative bolted connection with dual-
501 slot hole for modular steel buildings[J]. *Engineering Structures*, 2023, 279: 115619.
- 502 [3] Xiong M X, Liew J Y R. Experimental study to differentiate mechanical behaviours of TMCP
503 and QT high strength steel at elevated temperatures[J]. *Construction and Building Materials*, 2020,
504 242: 118105.
- 505 [4] Luo Z, Shi Y, Xue X, et al. Nonlinear patch resistance performance of hybrid titanium-clad
506 bimetallic steel plate girder with web opening[J]. *Journal of Building Engineering*, 2023, 65:
507 105703.
- 508 [5] Kang Z, Liao Q, Zhang Z, et al. Carbon neutrality orientates the reform of the steel industry[J].
509 *Nature Materials*, 2022, 21(10): 1094-1098.
- 510 [6] Hua J, Fan H, Xue X, et al. Tensile and low-cycle fatigue performance of bimetallic steel bars
511 with corrosion[J]. *Journal of Building Engineering*, 2021, 43: 103188.
- 512 [7] Hua J, Yang Z, Xue X, et al. Bond properties of bimetallic steel bar in seawater sea-sand
513 concrete at different ages[J]. *Construction and Building Materials*, 2022, 323: 126539.
- 514 [8] Hua J, Wang F, Xue X, et al. Post-fire ultra-low cycle fatigue properties of high-strength steel
515 via different cooling methods[J]. *Thin-Walled Structures*, 2023, 183: 110406.
- 516 [9] Jiang J, Bao W, Peng Z Y, et al. Experimental investigation on mechanical behaviours of TMCP
517 high strength steel[J]. *Construction and Building Materials*, 2019, 200: 664-680.
- 518 [10] Zhang Z, Xu Y, Huang Y, et al. Experiment study on the mechanical properties and constitutive
519 model of grade 1960 steel wires under and after elevated temperatures[J]. *Journal of Building*

520 Engineering, 2024, 82: 108318.

521 [11] Hua J, Wang F, Xue X, et al. Residual monotonic mechanical properties of bimetallic steel bar
522 with fatigue damage[J]. Journal of Building Engineering, 2022, 55: 104703.

523 [12] Wang W, Li S, Ran T. Numerical Study on High Strength Q690 Steel Flush End-Plate
524 Connections at Elevated Temperatures[J]. Fire Technology, 2024: 1-26.

525 [13] Xiong M X, Pi P W, Gong W, et al. Mechanical properties of TMCP high strength steels with
526 different strength grades at elevated temperatures[J]. Journal of Building Engineering, 2022,
527 48:103874.

528 [14] Wu Z, Li L, Wu R, et al. Determination of high-temperature creep and post-creep response of
529 structural steels[J]. Journal of Constructional Steel Research, 2022, 193: 107287.

530 [15] Kumar W, Sharma UK, Pathak P. Mechanical properties of low-alloyed YSt-355-FR (0.126%
531 Mo) cold-formed steel tube at elevated temperatures[J]. Journal of Constructional Steel Research,
532 2022, 192:107198.

533 [16] Li G Q, Lyu H, Zhang C. Post-fire mechanical properties of high strength Q690 structural
534 steel[J]. Journal of Constructional Steel Research, 2017, 132: 108-116.

535 [17] Hua J, Xue X, Huang Q, et al. Post-fire performance of high-strength steel plate girders
536 developing post-buckling capacity[J]. Journal of Building Engineering, 2022, 52: 104442.

537 [18] Xing Y, Wang W, Zhao O. Experimental, numerical and analytical studies on full-scale cold-
538 formed steel center-sheathed shear walls subjected to combined loading[J]. Engineering Structures,
539 2024, 307: 117910.

540 [19] Cao K, Zhai S Y, Lyu Y F, et al. Working mechanism evaluations of full-scale joints with
541 bolted-cover plate connection for modular steel buildings[J]. Thin-Walled Structures, 2024, 199:
542 111772.

543 [20] Wang W, Li Y, Wang Z, et al. Experimental and numerical study on the behavior of high
544 strength Q960 steel columns after fire exposure[J]. Thin-Walled Structures, 2024: 111748.

545 [21] Ren C, Dai L, Huang Y, et al. Experimental investigation of post-fire mechanical properties of
546 Q235 cold-formed steel[J]. Thin-Walled Structures, 2020, 150: 106651.

547 [22] Tao Z. Mechanical properties of prestressing steel after fire exposure[J]. Materials and
548 Structures, 2015, 48: 3037-3047.

549 [23] Lu J, Liu H, Chen Z. Post-fire mechanical properties of low-relaxation hot-dip galvanized

550 prestressed steel wires[J]. *Journal of Constructional Steel Research*, 2017, 136: 110-127.

551 [24] Zhang L, Wei Y, Au F T K, et al. Mechanical properties of prestressing steel in and after fire[J].
552 *Magazine of Concrete Research*, 2017, 69(8): 379-388.

553 [25] Du Y, Peng J, Liew J Y R, et al. Mechanical properties of high tensile steel cables at elevated
554 temperatures[J]. *Construction and Building Materials*, 2018, 182: 52-65.

555 [26] Gao X, Zhang X, Liu H, et al. Residual mechanical properties of stainless steels S30408 and
556 S31608 after fire exposure[J]. *Construction and Building Materials*, 2018, 165: 82-92.

557 [27] Shi G, Wang S, Chen X, et al. Post-fire mechanical properties of base metal and welds of Q235
558 steel[J]. *Journal of Constructional Steel Research*, 2021, 183: 106767.

559 [28] Qiang X, Bijlaard F S K, Kolstein H. Post-fire mechanical properties of high strength structural
560 steels S460 and S690[J]. *Engineering Structures*, 2012, 35: 1-10.

561 [29] Qiang X, Bijlaard F S K, Kolstein H. Post-fire performance of very high strength steel S960[J].
562 *Journal of Constructional Steel Research*, 2013, 80: 235-242.

563 [30] Lee J, Engelhardt M D, Taleff E M. Mechanical properties of ASTM A992 steel after fire[J].
564 *Engineering Journal*, 2012, 49(1): 33.

565 [31] Wang W, Liu T, Liu J. Experimental study on post-fire mechanical properties of high strength
566 Q460 steel[J]. *Journal of Constructional Steel Research*, 2015, 114: 100-109.

567 [32] Zhou H, Wang W, Wang K, et al. Mechanical properties deterioration of high strength steels
568 after high temperature exposure[J]. *Construction and Building Materials*, 2019, 199: 664-675.

569 [33] Huang D, Zhang L, Wang W, et al. Test on post-fire residual mechanical properties of high
570 strength Q690 steel considering tensile stress in fire[J]. *Journal of Constructional Steel Research*,
571 2022, 194: 107340.

572 [34] Yu Y, Lan L, Ding F, et al. Mechanical properties of hot-rolled and cold-formed steels after
573 exposure to elevated temperature: A review[J]. *Construction and Building Materials*, 2019, 213:
574 360-376.

575 [35] Li Y, Wang M, Li G, et al. Mechanical properties of hot-rolled structural steels at elevated
576 temperatures: a review[J]. *Fire Safety Journal*, 2021, 119: 103237.

577 [36] Huang D, Kodur V, Wang W. Temperature-dependent properties of high-strength steel for
578 evaluating the fire resistance of structures[J]. *Advances in Structural Engineering*, 2023, 26(12):
579 2265-2281.

- 580 [37] Chiew S P, Zhao M S, Lee C K. Mechanical properties of heat-treated high strength steel under
581 fire/post-fire conditions[J]. Journal of Constructional Steel Research, 2014, 98: 12-19.
- 582 [38] Gunalan S, Mahendran M. Experimental investigation of post-fire mechanical properties of
583 cold-formed steels[J]. Thin-Walled Structures, 2014, 84: 241-254.
- 584 [39] Wang W, Zhang Y, Xu L, et al. Mechanical properties of high-strength Q960 steel at elevated
585 temperature[J]. Fire Safety Journal, 2020, 114: 103010.
- 586 [40] GB/T 19879, Steel plates for building structures, Standards Press of China, Beijing, 2023 (in
587 Chinese).
- 588 [41] GB/T 228, 1 Metallic Materials-Tensile Testing Part 1: Method of Test at Room Temperature,
589 Standards Press of China, Beijing, 2010 (in Chinese).
- 590 [42] GB/T 228, 2 Metallic Materials-Tensile Testing Part 2: Method of Test at Elevated Temperature,
591 Standards Press of China, Beijing, 2015 (in Chinese).
- 592 [43] Li S, Li A, Wang W. Mechanical properties and constitutive models of Q460GJ steel at elevated
593 temperatures [J]. Journal of Constructional Steel Research, under review.
- 594 [44] American Iron and Steel Institute (AISI), S100-16, North American Specification for the
595 Design of Cold-Formed Steel Structural Members, 2020.